Probing dark energy in the scope of a Bianchi type I spacetime

Hassan Amirhashchi[*]

Department of Physics, Mahshahr Branch, Islamic Azad University, Mahshahr 6351977439, Iran

(Received 2 December 2017; published 15 March 2018)

It is well known that the flat Friedmann-Robertson-Walker metric is a special case of Bianchi type I spacetime. In this paper, we use 38 Hubble parameter, $H(z)$, measurements at intermediate redshifts $0.07 \leq z \leq 2.36$ and its joint combination with the latest "joint light curves" (JLA) sample, comprising 740 type Ia supernovae in the redshift range of $z\epsilon[0.01, 1.30]$ to constrain the parameters of the Bianchi type I dark energy model. We also use the same datasets to constrain flat a ΛCDM model. In both cases, we specifically address the expansion rate H_0 as well as the transition redshift z_t determinations out of these measurements. In both models, we found that using joint combination of datasets gives rise to lower values for model parameters. Also to compare the considered cosmologies, we have made Akaike information criterion and Bayes factor (Ψ) tests.

DOI: 10.1103/PhysRevD.97.063515

I. INTRODUCTION

Using supernovae type Ia (SNe Ia) as standard candles enabled us to probe the history of cosmic expansion at high accuracy, i.e., at low and intermediate redshifts. Observations from various independent research teams show that the expansion of our universe is speeding up at present time [1–5]. This phase transition from decelerating to accelerating expansion is due to an unknown mechanism changing the sign of the universal deceleration parameter $q(z)$. In spite of considerable efforts, still the correct physical explanation of such transition is one of the most challenging fields in cosmology. However, it is commonly accepted that the current cosmic acceleration could be investigated (1) by assuming an unknown and unusual source of energy with negative pressure called dark energy (DE) in cosmic fluid or (2) by assuming the general theory of gravity is modified. Within the framework of general relativity (GR), the simplest way for explaining such a mechanism is by assuming a cosmological constant Λ [6,7] in Einstein field equations. However, this scenario suffers from cosmological and coincidence problems [8–10]. Exploring DE is possible through its equation of state parameter (EoS) connecting pressure and density of DE as $p = \omega^X \rho$ (where p is the pressure and ρ is the density of DE) as well as its microphysics, characterized by the speed of sound c_s^2. It is worth mentioning that the study of a fluid model of dark energy requires considering both an EoS and sound speed c_s^2 at the same time. As mentioned by Sandage [11] in both static and dynamical cases, the basic characteristics of the cosmological evolution could be expressed in terms of the Habble (H_0) and deceleration (q_0) parameters, which enable us to construct model-independent kinematics of the cosmological expansion.

Long time (since 1929) measurements of the Hubble constant, H_0, indicated that the value of this parameter was between 50 and 100 km s^{-1}/Mpc [12,13]. Improving the control of systematics, use of different and novel calibration techniques, and the aid of space facilities, now we can estimate the observed value of H_0 more accurately. Comparing different observation techniques indicates that the indirect estimates of the Hubble constant lead to lower values of H_0 compared with direct estimations. For example, the most recent direct estimate of H_0 obtained by Riess *et al.* [14] is $H_0 = (73.0 \pm 1.8)$ km s^{-1}/Mpc, whereas the indirect measurement of the expansion rate of our universe, such as the observations of the cosmic microwave background (CMB) anisotropy by WMAP [15], Planck Collaboration [16] and the joint Atacama Cosmology Telescope (ACT) [17], and the WMAP 7-year CMB anisotropy data [18] yielded $H_0 = (70.0 \pm 2.2)$ km s^{-1}/Mpc, $H_0 = (67.27 \pm 0.66)$ kms^{-1}/Mpc, and $H_0 = (70.0 \pm 2.4)$ km s^{-1}/Mpc, respectively. The best technique for deriving a convincing summary observational estimate of H_0 is the median statistics technique [19–25]. Applying median statistics to 331 H_0 estimates listed by Huchra,[1] Gott *et al.* [19] obtained $H_0 = (67 \pm 3.5)$ km s^{-1}/Mpc. From 461 measurements (up to the middle of 2003), Chen *et al.* [21] found $H_0 = (68 \pm 3.5)$ km s^{-1}/Mpc, and from 553 measurements (up to early 2011), Chen and& Ratra [26,27] found $H_0 = (68 \pm 2.8)$ km s^{-1}/Mpc. It is worth noting that because the expansion rate of the universe, H_0, is degenerate with the SN absolute magnitude, the observations of SN Ia

[*]h.amirhashchi@mhriau.ac.ir, hashchi@yahoo.com

[1]https://www.cfa.harvard.edu/dfabricant/huchra/.

by themselves could not evaluate a value for the local expansion rate of the universe. However, as proposed by Jimenez *et al.* [28], passively evolving red galaxies whose age can be precisely estimated from a spectroscopic analysis could be used to provide the redshift dependence of the cosmic expansion rate $H(z)$. Liu *et al.* [29] have recently used these observational Hubble data (OHD) and found a value of $H_0 = (68.6)\ \mathrm{km\,s^{-1}/Mpc}$. It should be emphasized that more care has to be taken when one uses several SN datasets such as union as these datasets provide cosmological distance moduli that are derived assuming a flat ΛCDM model. Hence, to constrain cosmological models that are different from ΛCDM, we can use "latest joint light curves" (JLA) dataset[2] which provides model-independent apparent magnitudes instead of model-dependent distance moduli. Recently, Lukovic *et al.* [30] have used the JLA dataset to constrain a different class of models based on the Lemaître-Tolman-Bondi (LTB) metric. The reader is advised to see Refs. [31–35] for more detailed study of LTB spacetime. In this paper, we consider $38 H(z)$ data points at the redshift range of $0.07 < z < 2.36$ compiled by Farooq and Ratra [36], the JLA dataset, and their combination to constrain different models based on Bianchi type I (henceforth BI) metric that describes a homogeneous but anisotropic universe.

The plan of the paper is as follows. Section II deals with the theoretical models we considered. In Sec. III, we briefly summarize the data analysis method we use. In Sec. III A, we constrain the ΛCDM model. We constrain the ωBI model in Sec. III B. We derive the transition redshift for both models in Sec. III C. Finally, in Sec. IV, we summarize our findings and conclusions.

II. THEORETICAL MODELS

The assumption of considering spacetime to be homogeneous and isotropic (cosmological principle) could suffer due to the following two facts. First, is the recent cosmic observations which indicate small variations between the intensities of the microwaves coming from different directions in the sky. Second, is the fact that at very large scales (beyond event horizon) and also at the small scales the universe necessarily does not have the same symmetries as we consider for Friedmann-Robertson-Walker (FRW) spacetime. Therefore, it will be more reasonable to obtain "almost FRW" models representing a universe that is "FRW-like" on large scales but allows for generic inhomogeneities and anisotropies to arise during structure formation on a small scale. To be able to compare detailed observations, we take the Bianchi type I (BI) metric which is homogeneous but anisotropic. It is shown by Goliath and Ellis [37] that some Bianchi models isotropize due to inflation.

[2]All data used are available on http://supernovae.in2p3.fr/sdss-snls-jla/ReadMe.html.

In an orthogonal form, the Bianchi type I line element is given by

$$ds^2 = -dt^2 + A^2(t)dx^2 + B^2(t)dy^2 + C^2(t)dz^2, \quad (1)$$

where $A(t)$, $B(t)$, and $C(t)$ are functions of time only.

Einstein's field equations (in gravitational units of $8\pi G = c = 1$) read as

$$R^{\mu}_{\nu} - \frac{1}{2} R g^{\mu}_{\nu} = T^{(m)\mu}_{\nu} + T^{(X)\mu}_{\nu}, \quad (2)$$

where $T^{(m)\mu}_{\nu}$ and $T^{(X)\mu}_{\nu}$ are the energy momentum tensors of dark matter and dark energy, respectively. These are given by

$$\begin{aligned} T^{m\mu}_{\nu} &= \mathrm{diag}[-\rho^m, p^m, p^m, p^m], \\ &= \mathrm{diag}[-1, \omega^m, \omega^m, \omega^m]\rho^m, \end{aligned} \quad (3)$$

and

$$\begin{aligned} T^{X\mu}_{\nu} &= \mathrm{diag}[-\rho^X, p^X, p^X, p^X], \\ &= \mathrm{diag}[-1, \omega^X, \omega^X, \omega^X]\rho^X, \end{aligned} \quad (4)$$

where (ρ^m, p^m) and (ρ^X, p^X) are the energy density and pressure of the dark matter (DM) and dark energy (DE), respectively. Energy density and pressure of each component are related by the EoS, $p = \omega\rho$. The 4-velocity vector $u^i = (1, 0, 0, 0)$ is assumed to satisfy $u^i u_j = -1$. As shown in Refs. [38,39], the exact solution of Einstein's field equations in a comoving coordinate system ($u^i = \delta^i_0$) leads to the following Friedmann-like equations:

$$\left(\frac{\dot{a}}{a}\right)^2 = \frac{1}{3}\sum_i \rho_i + K a^{-6}, \qquad K < 0, \quad (5)$$

$$\frac{\ddot{a}}{a} = -\frac{1}{6}\sum_i \rho_i (1 + 3\omega_i), \quad (6)$$

where $a = (ABC)^{\frac{1}{3}}$ is the average scale factor. In terms of the anisotropy parameter, A_m, Eq. (5) could be written as follows (see the Appendix):

$$\left(\frac{\dot{a}}{a}\right)^2 = \frac{1}{3}\sum_i \rho_i + \frac{A_m}{6}. \quad (7)$$

It is worth mentioning that the constant K also is a scale that denotes the deviation from isotropy; therefore, $K = 0$ (and equivalently $A_m = 0$) represents the flat FRW universe. From Eq. (6), it is clear that to obtain accelerated expansion (i.e., $\ddot{a} > 0$), at least one of the components of the cosmic fluid must have $\omega < -\frac{1}{3}$. Using Eq. (6), one can find the dimensional Hubble parameter as

$$E(z) = \frac{H}{H_0} = \sqrt{\sum_i \Omega_i (1+z)^{3(1+\omega_i)} + \tilde{A}_m}, \qquad (8)$$

where $H(0) = H(z=0)$, $\tilde{A}_m = (\frac{A_m}{6})H_0^2$, and $\Omega_i = 3H_0^2\rho_i$ is the current density of the ith component. Also the law of energy-conservation equation ($T^{\mu\nu}_{;\nu} = 0$) yields

$$\sum_i \dot{\rho}_i + 3(1+\omega_i)\rho_i H = 0, \qquad (9)$$

which shows the density evolution of each component of the cosmic fluid. While we consider various EoS parameters for the DE models, the DM is usually considered cold with zero EoS parameter ($\omega^m = 0$). In our study, we discuss the observational constraints on the free parameters of the following models.

Model I. We consider flat ΛCDM with $\omega^X = -1$, which could be obtained by putting $K = 0$ in Eq. (6). This is the simplest way of best fitting current cosmological observations. The base parameter set for Model I is

$$\mathbf{P} = \{\Omega^{X\equiv\Lambda}, \Omega^m, n_s, H_0, Age/Gyr, \sigma_8\}.$$

Model II. We also consider a ωBI model with a EoS parameter that is constant with respect to the cosmic expansion. In this case, the best set of parameters is

$$\mathbf{P} = \{\Omega^X, \Omega^m, n_s, H_0, Age/Gyr, \sigma_8, A_m, \omega^X\}.$$

III. DATA SETS AND RESULTS

The main goal of this paper is to constrain the free parameters of the theoretical models described above using independent observables that are SN Ia (JLA dataset), OHD, and their joint combination which could increase the sensitivity of our estimates. We specifically address the H_0 determination out of these measurements. In this section, we briefly describe the observational data sets used in this work.

SN Ia: As mentioned above, the best advantage of the JLA dataset is the model-independent property of this dataset. The JLA dataset we consider in this paper comprises 740 type Ia supernovae in the redshift range of $0.01 \le z \le 1.30$ [40]. To calculate the corresponding likelihood (L_{SN}) and hence constrain the model parameters, we follow the method given by Trøst Nielsen *et al.* [41]. Note that, in analyzing the JLA dataset by itself, we do not consider any prior H_0. As we will show below, the JLA dataset by itself is not sensitive to H_0. However, in the joint analysis, JLA affects the estimate of H_0.

OHD: Farooq and Ratra have recently compiled $38H(z)$ data points in the redshift range of $0.07 \le z \le 2.36$ [36]. To constrain cosmological parameters, we use this dataset and maximize the following likelihood.

$$L_{\mathrm{OHD}} \propto \exp\left[-\frac{1}{2}\sum_{i=1}^{38}\left(\frac{H^{th}(z_i, \mathbf{P}) - H^{\mathrm{obs}}(z_i)}{\sigma_{H,i}^2}\right)^2\right], \qquad (10)$$

where H^{th} is the predicted value of $H(z)$ in the cosmological model given by Eq. (7), $H^{\mathrm{obs}}(z_i)$ is the measured value with variance $\sigma_{H,i}^2$ at redshift z_i, and $\mathbf{P}$ represents the free parameters of the cosmological model.

Combined analysis: In what follows, we show that both JLA and OHD datasets provide good estimates of the cosmological parameters. However, to obtain more stringent constraints, we combine both datasets. One of the advantage of combining datasets is that the joint analysis allows us to provide separate estimates for the absolute magnitude of SN and the Hubble constant $H(z)$. To evaluate the total likelihood as the product of the likelihoods of the single s, we assume that the datasets are independent. The total likelihood is given by

$$L_{\mathrm{tot}} = L_{\mathrm{SN}} L_{\mathrm{OHD}}. \qquad (11)$$

To obtain correlated Markov Chain Monte Carlo (MCMC) of the samples, we modify CLASS [42] and Monte Python [43] codes and use Metropolis Hastings algorithm with uniform priors on the model parameters. To analyze the MCMC chains, we use the GetDist Python package [44].

A. Constraints on a flat ΛCDM model

The flat ΛCDM model which is commonly considered as the concordance model in cosmology is the simplest model for the best fitting of current observations. Therefore, this model has been tested with almost all the available cosmological observables. In this case, the results of our statistical analysis are shown in Table I. The contour plots of the Model I parameters are also depicted in Fig. 1. From Table I, we observe that our values for Ω^m (at 1σ error), obtained from OHD and OHD + JLA, are in good agreement with those from the recent determination of Planck: TT, TE, EE + lowP, which provided $\Omega^m = 0.316 \pm 0.009$.

Moreover, our estimates for the current expansion rate, H_0, derived from OHD alone and OHD + JLA are in good agreement with those obtained by Chen and& Ratra (68 ± 2.8) [26], Ade *et al.*, Planck (67.8 ± 0.9) [45], and Aubourg *et al.*, BAO (67.3 ± 1.1) [46]. It is worth

TABLE I. Results from the fits of the ΛCDM model to the data at 1σ confidence level.

Parameter	JLA	OHD	JLA + OHD
H_0	⋯	68.3 ± 1.5	67.9 ± 1.2
Ω^Λ	0.624 ± 0.031	0.6890 ± 0.0076	0.687 ± 0.012
Ω^m	0.376 ± 0.031	0.3110 ± 0.0076	0.313 ± 0.012
n_s	0.959 ± 0.019	0.9671 ± 0.0043	0.9662 ± 0.0057
σ_8	0.835 ± 0.042	0.828 ± 0.015	0.829 ± 0.015
Age/Gyr	$13.808^{+0.039}_{-0.035}$	13.794 ± 0.046	$13.803^{+0.031}_{-0.027}$

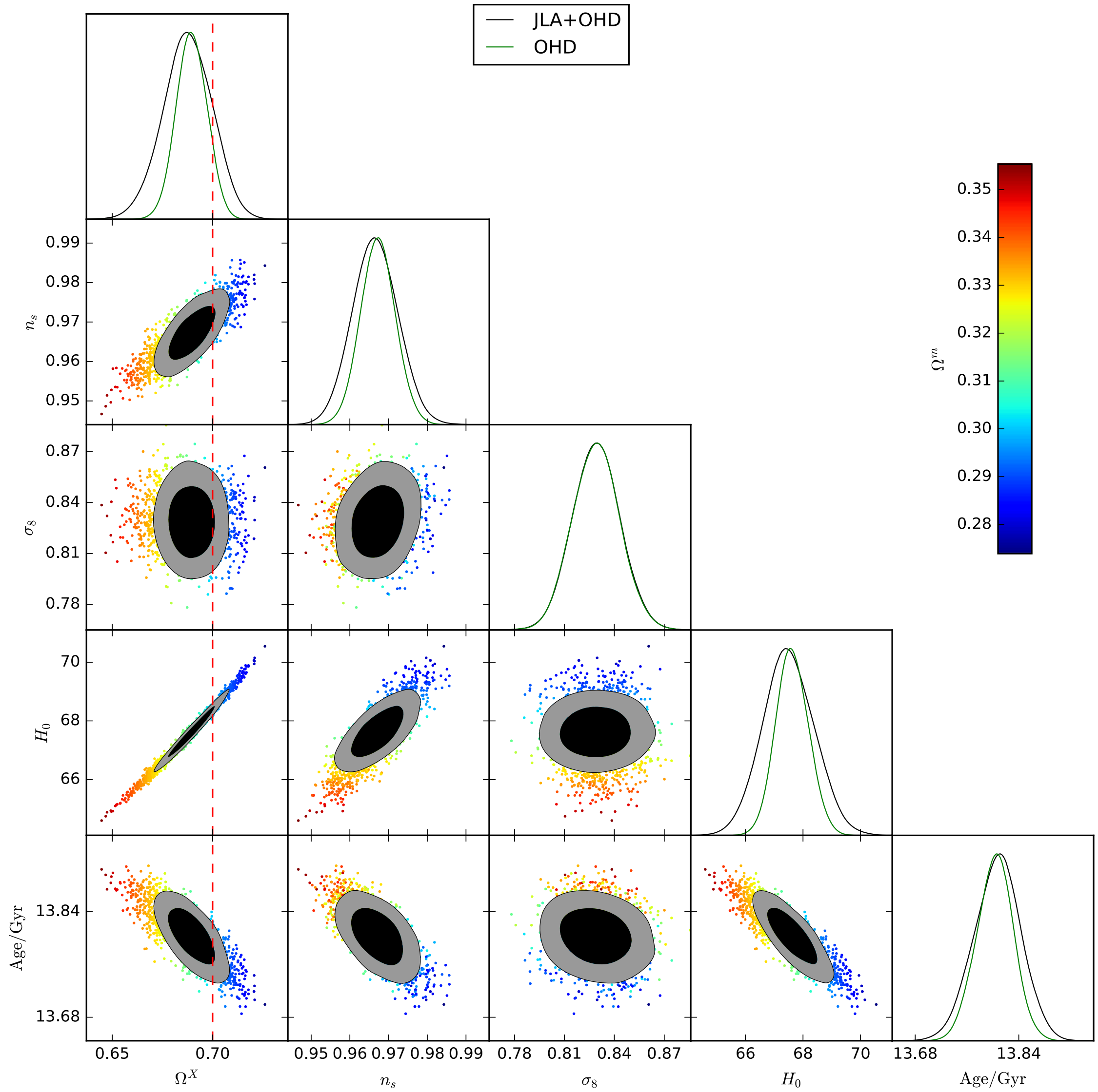

FIG. 1. One-dimensional marginalized distribution and two-dimensional contours with 68% CL and 95% CL for the model parameters. The vertical dotted red line stands for $\Omega^\Lambda = 0.7$.

mentioning that although the final value for H_0 derived from the joint JLA + OHD analysis is in good agreement with that of Planck (2015) and BAO (see Fig. 2), its difference from the findings by Efstathiou [47] and Riess *et al.* [14] is by 1.9σ and 2.6σ, respectively. It is important to note that the JLA dataset by itself is not sensitive to the expansion rate H_0, but when we combine it with the other datasets, in the joint analysis, JLA constrains other parameters of the model under consideration, which in turn affects the estimate of H_0. The robustness of our fits can be viewed by looking at Figs. 2 and 3. From these figures, we observe that the joint analysis gives rise to a better fit to the observational data.

B. Constraints on the ωBI model

The ωBI model considers two more free parameters, a DE fluid with a free EoS parameter ω with $-1 < \omega < -\frac{1}{3}$, which we assume to be constant with respect to the cosmic expansion, and a constant parameter α, which is responsible for the inherent anisotropy of the BI spacetime. Table II shows the results of our statistical analysis for Model II. Figure 4 depicts 1σ and 2σ confidence regions from the fits of the ωBI model to the OHD and OHD + JLA datasets. Table II shows that the matter density Ω^m derived from Model II by using OHD and the joint analysis (OHD + JLA) is again in good agreement with the value obtained from the Planck 2015 Collaboration. Also, although the estimates of the current expansion rate H_0 derived from OHD alone and the joint OHD + JLA analysis are in excellent agreement with results of Refs. [45,46] but still are different from the results of Efstathiou [47] and Riess *et al.* [14] by 2.1σ and 2.9σ, respectively. The robustness of our fits can be viewed by looking at Figs. 5 and 6.

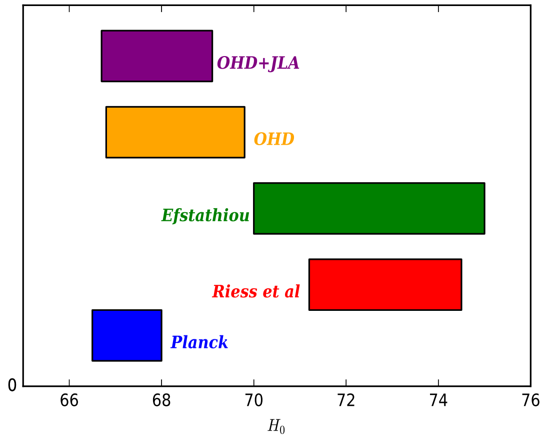

FIG. 2. Schematic representation at 1σ CL of H_0 for Model I when fitted to OHD (gold) and two datasets combined (purple). Constraints from the direct measurement by Riess *et al.* [14] (red), the reanalysis by Efstathiou [47] (green), and the Planck Collaboration [16] (blue) are also shown.

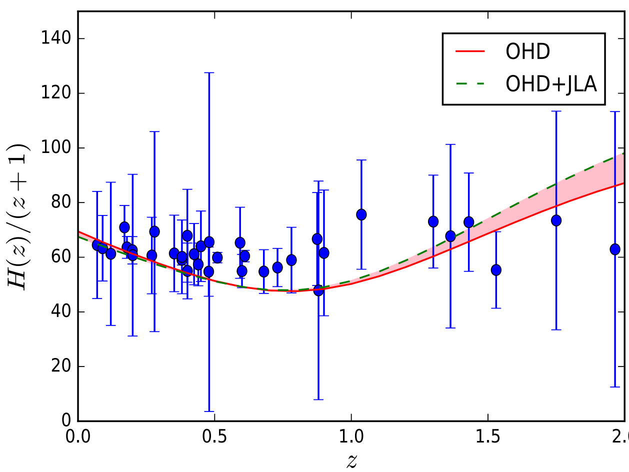

FIG. 3. Hubble rate of Model I (flat ΛCDM represents the case where $\alpha = 0$ and $\omega = -1$) versus the redshift z. The points with bars indicate the experimental data summarized in Table I of Ref. [36]. It is clear that Model I is best fitted to data when we use joint analysis of two datasets.

In what follows, we use the Akaike information criterion (AIC) and Bayes factor (Ψ) in order to compare the considered cosmologies. For a given theoretical model and a given dataset, the Akaike estimate of minimum information (Akaike 1974) [48] is defined as

$$\mathrm{AIC} = -2\log L^{\max} + 2N, \qquad (12)$$

where N is the number of independent parameters of the model. In this method, the preference is given to the model with the lowest AIC. Similarly, we use the Bayes factor Ψ which provides a criterion for choosing between two models by comparing their best likelihood values. It is worth noting that $0 \leq \Delta(\mathrm{AIC}) \leq 2$ gives substantial evidence for the model. $\Delta(\mathrm{AIC}) \leq 7$ shows less support for the model, and $\Delta(\mathrm{AIC}) > 10$ indicates that the model is unlikely. Here we are interested in comparing Model II (ωBI) with Model I (ΛCDM). Moreover, the Bayes factor, $\Psi = L^{\max}_{\Lambda\mathrm{CDM}}/L^{\max}_{\omega\mathrm{BI}}$, represents the odds for the ΛCDM model against the ωBI model. We note that odds lower than 1:10 indicate a strong evidence against the ΛCDM model, whereas odds greater than 10:1 indicate strong evidence against the ωBI model (Jeffreys [49]). The difference, $\Delta(\mathrm{AIC}) = AIC_{\omega\mathrm{BI}} - AIC_{\Lambda\mathrm{CDM}}$, of the AIC value and the Bayes factor Ψ of the ωBI scenario against ΛCDM are shown in Table III. The values of $-2\log L$ for ωBI and ΛCDM models when we fitted them to the OHD data alone are found to be 27.35 and 28.03, respectively, which clearly shows that ωBI can be used to fit OHD data. This result is in agreement with that obtained by Wang and Zhang [50]. Also, fitting both models to the JLA data alone, we obtain $-2\log L_{\omega\mathrm{BI}} = -212.53$ and $-2\log L_{\Lambda\mathrm{CDM}} = -213.96$, which shows that ωBI can be used to fit the SN Ia data, as well. The differences, $\Delta(\mathrm{AIC})$, of the AIC values as well as the Bayes factor Ψ are presented in Table III.

TABLE II. Results from the fits of the ωBI model to the data at 1σ confidence level.

Parameter	JLA	OHD	JLA + OHD
H_0	$\cdots$	67.94 ± 1.6	67.53 ± 1.1
Ω^X	0.624 ± 0.031	0.6920 ± 0.0052	0.6862 ± 0.0092
Ω^m	0.376 ± 0.031	0.310 ± 0.0052	0.3120 ± 0.0092
n_s	0.959 ± 0.019	0.9663 ± 0.0023	0.9648 ± 0.0046
σ_8	0.826 ± 0.021	0.825 ± 0.018	0.823 ± 0.052
Age/Gyr	$14.018^{+0.035}_{-0.075}$	13.812 ± 0.046	13.815 ± 0.031
A_m	0.008 ± 0.005	0.006 ± 0.007	0.002 ± 0.004
ω^X	-0.91 ± 0.65	-0.96 ± 0.83	-0.97 ± 0.35

C. Cosmological deceleration-acceleration transition redshift

It is well known that the expansion phase of the universe changes from decelerating to accelerating at a specific redshift called "transition redshift" z_t. Here, for completeness of our study, we derived z_t for both models by using OHD and combined OHD + JLA datasets. In general, the deceleration parameter is given by

$$q(z) = -\frac{1}{H^2}\left(\frac{\ddot{a}}{a}\right) = \frac{(1+z)}{H(z)}\frac{dH(z)}{dz} - 1. \qquad (13)$$

It is clear that the transition redshift is implicitly defined by the condition $q(z_t) = \ddot{a}(z_t) = 0$. From (7), one could easily find the transition redshift for Model I as

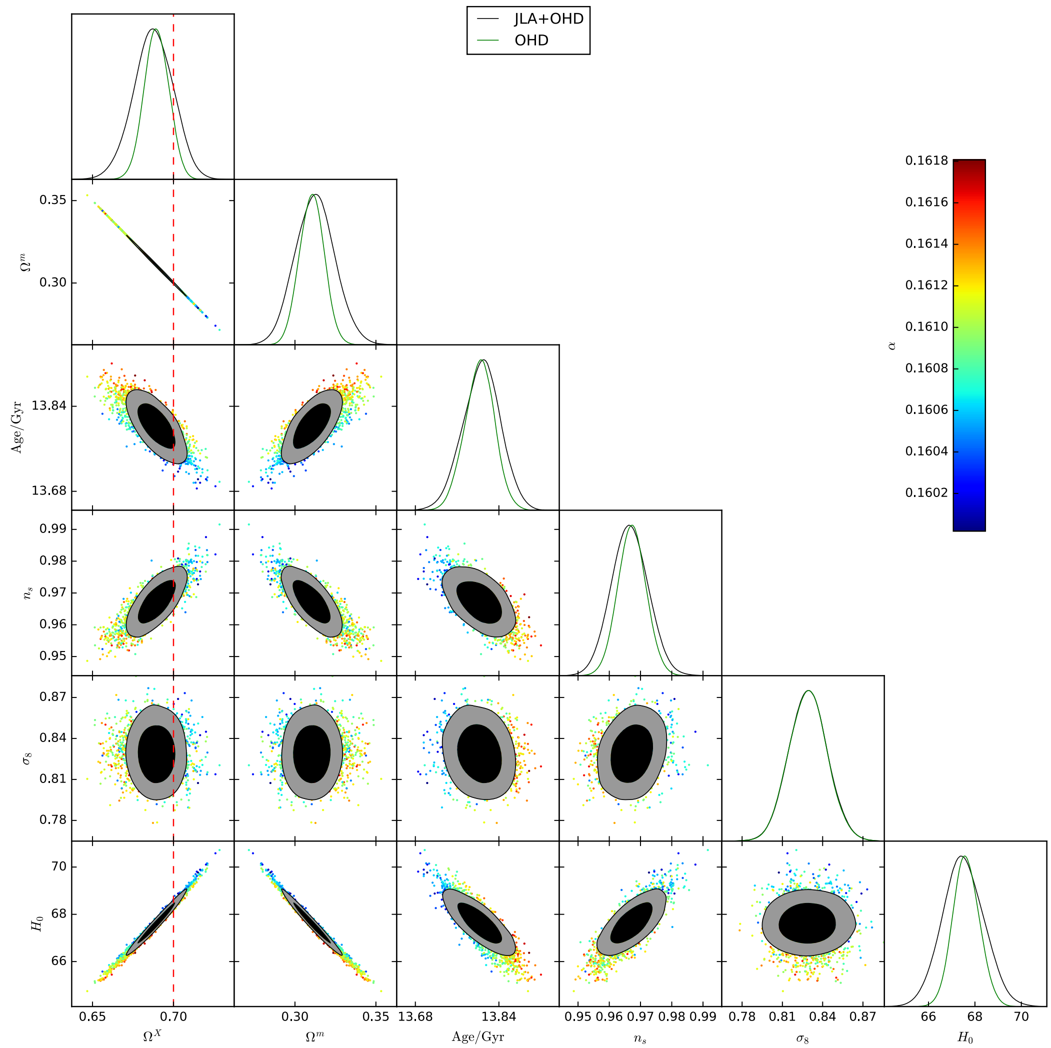

FIG. 4. 1σ and 2σ confidence regions from the fits of the ωBI model to the single OHD and the joint OHD + JLA analysis. The vertical dotted red line stands for $\Omega^X = 0.7$.

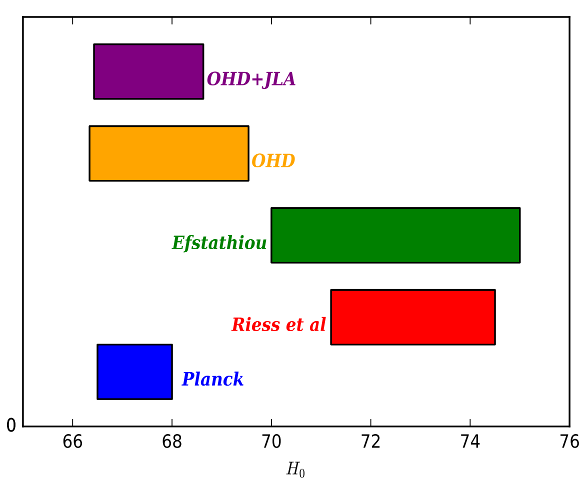

FIG. 5. Schematic representation at 1σ confidence region of H_0 for Model II when fitted to OHD (gold) and the joint OHD + JLA (purple). Constraints from other measurements are shown.

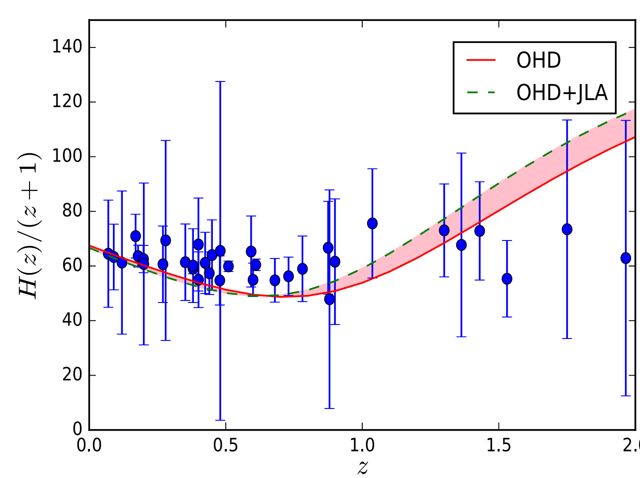

FIG. 6. Hubble rate of Model II (ωBI) represents the case when $\alpha \neq 0$ and $-1 < \omega < -\frac{1}{3}$ versus the redshift z. This model is best fitted to data when we use joint analysis of two datasets.

TABLE III. Comparison of the cosmological models by $\Delta(\mathrm{AIC})$ and Ψ using the joint OHD + JLA dataset.

Model	$\Delta(\mathrm{AIC})$	Ψ
ΛCDM	0	1
ωBI	1.27	1:1.18

TABLE IV. Deceleration parameters and deceleration-acceleration transition redshifts.

Model	z_t(OHD)	z_t(OHD + JLA)
ΛCDM	0.642 ± 0.0155	0.637 ± 0.0244
ωBI	0.671 ± 0.0185	0.639 ± 0.0283
$q_{\Lambda\mathrm{CDM}}$	$-5.43^{+0.38}_{-0.59}$	$-5.56^{+0.49}_{-0.35}$
$q_{\omega\mathrm{BI}}$	$-5.79^{+0.37}_{-0.45}$	$-6.10^{+0.67}_{-0.21}$

$$z_t = \left(\frac{2\Omega^\Lambda}{\Omega^m}\right)^{\frac{1}{3}} - 1. \qquad (14)$$

Also, from (7), the transition redshift for the ωBI model could be found as

$$z_t = \left(\frac{\Omega^m}{(\Omega^m - 1)(1 + 3\omega^X)}\right)^{\frac{1}{3\omega^X}} - 1. \qquad (15)$$

Using the best-fit parameters given in Tables II and III, we can obtain the transition redshift for ΛCDM and ωBI models. The deceleration parameter as well as the deceleration-acceleration transition redshift with corresponding standard deviation for each model are shown in Table IV. From this table, we observe that, in both models, combining two datasets gives rise to more stringent

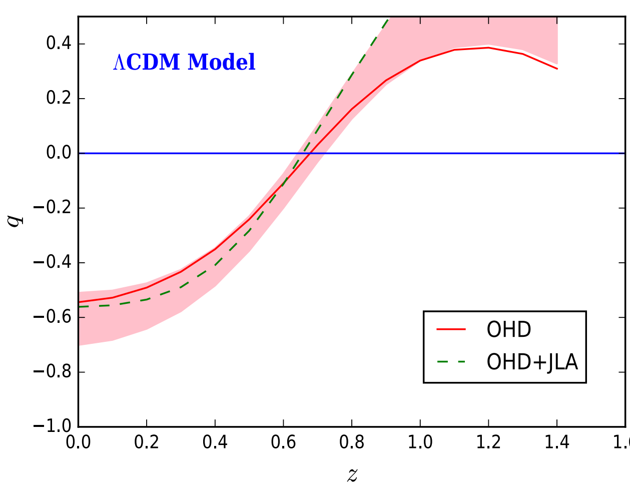

FIG. 7. Variation of deceleration parameter q versus redshift z for ΛCDM model by using OHD and OHD + JLA datasets. When we constrain the model by joint OHD + JLA analysis, it enters the accelerating phase at lower redshift.

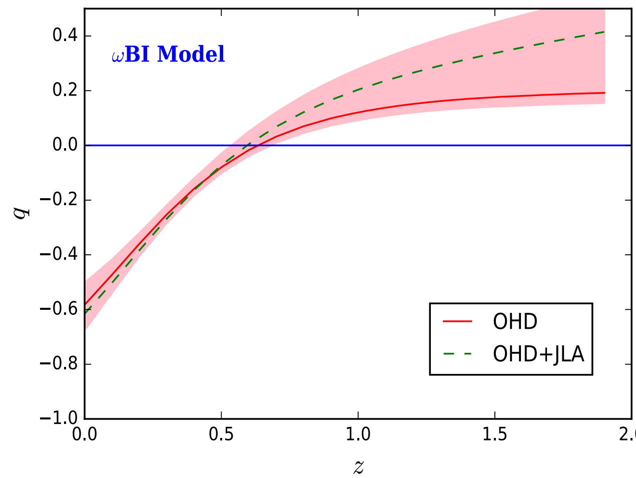

FIG. 8. Variation of deceleration parameter q versus redshift z for the ωBI model by using OHD and OHD + JLA datasets. When we constrain the model by joint OHD + JLA analysis, it enters the accelerating phase at lower redshift.

constraints on the transition redshift. These results show that the ωBI model enters the accelerating phase at an earlier time with respect to the ΛCDM model. However, in both models, when we use joint OHD + JLA analysis to constrain model parameters, the transition to accelerating phase occurs at lower redshifts. Figures 7 and 8 depict the variation of deceleration parameter q versus redshift z for both models and different datasets.

IV. CONCLUDING REMARKS

Instead of maximally symmetric FRW spacetime, we considered Bianchi type I metric which is homogeneous but anisotropic. Based on recent cosmic observations, this metric is more consistent with the line element of the real universe. Two datasets, namely observational Hubble data (OHD) and "latest joint light curves" (JLA) and their joint combination have been considered to constrain parameters of two theoretical ΛCDM and ωBI models. In general, we found that using joint OHD + JLA dataset puts tighter constraints on the model parameters. Specially, by using joint OHD + JLA, the expansion rate of universe is obtained as 67.9 ± 1.2 and 67.53 ± 1.1 for ΛCDM and ωBI models, respectively. These results are obviously in excellent agreement with results obtained by cosmic microwave background (CMB) anisotropies [45,51] and baryon acoustic oscillation (BAO) [46] projects. Other results, in particular, the current value of the deceleration parameter q_0 and its corresponding value of the transition redshift z_t for both models, are found to be in good agreement with almost all recent cosmological observations.

ACKNOWLEDGMENTS

The Mahshahr branch, Islamic Azad University, is thanked for providing facility and support where this work was carried out. The author is also grateful to the anonymous referee for valuable comments and suggestions.

APPENDIX: ANISOTROPY OF BIANCHI TYPE I SPACETIME

It have been shown in Refs. [35,36] that if we solve Einstein's field equations (2) for line element (1), the metric components could be obtained as

$$A(t) = a_1 a \exp\left(b_1 \int a^{-3} dt\right), \tag{A1}$$

$$B(t) = a_2 a \exp\left(b_2 \int a^{-3} dt\right), \tag{A2}$$

$$C(t) = a_3 a \exp\left(b_3 \int a^{-3} dt\right), \tag{A3}$$

where

$$a_1 a_2 a_3 = 1, \qquad b_1 + b_2 + b_3 = 0.$$

The anisotropy parameter A_m and the average Hubble parameter H are defined as

$$A_m = \frac{1}{3}\left[\left(\frac{H_x - H}{H}\right)^2 + \left(\frac{H_y - H}{H}\right)^2 + \left(\frac{H_z - H}{H}\right)^2\right], \tag{A4}$$

and

$$H = \frac{1}{3}(H_x + H_y + H_z), \tag{A5}$$

where directional Hubble parameters H_x, H_y, and H_z could be obtained as below:

$$H_x = \frac{\dot{A}(t)}{A(t)} = (1 - 3b_1 a^{-3})\frac{\dot{a}}{a}, \tag{A6}$$

$$H_y = \frac{\dot{B}(t)}{B(t)} = (1 - 3b_2 a^{-3})\frac{\dot{a}}{a}, \tag{A7}$$

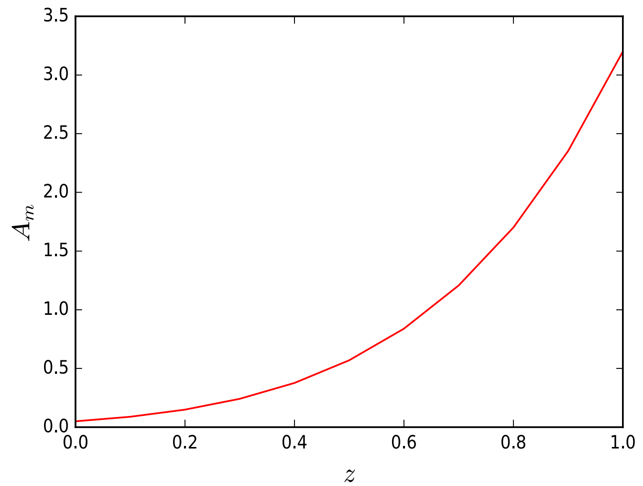

FIG. 9. Variations of anisotropy parameter A_m versus redshift z.

$$H_z = \frac{\dot{C}(t)}{C(t)} = (1 - 3b_3 a^{-3})\frac{\dot{a}}{a}. \tag{A8}$$

Using Eqs. (A6)–(A8) and (A5) in Eq. (A4), we can find the expression of the anisotropy parameter as

$$A_m = 3a^{-6}(b_1^2 + b_2^2 + b_3^2). \tag{A9}$$

Because $K = b_1 b_2 + b_1 b_3 + b_2 b_3$ (see Ref. [36]), the above equation could be written in the following compact form:

$$A_m = -6Ka^{-6}. \tag{A10}$$

Note that K is a negative parameter. Equation (A10) clearly shows that as the universe expands, the anisotropy of Bianchi type I spacetime decreases and ultimately dies out at a redshift of $z = -1$ (the current value of anisotropy parameter is $A_m = -6K$. (See Fig. 9 for more details.) It is worth noting that to get FRW cosmology [(i.e., $A(t) = B(t) = C(t)$], one has to consider $b_1 = b_2 = b_3 = 0$, which leads to zero anisotropy parameter (i.e., $A_m = 0$).

[1] S. Perlmutter *et al.*, Nature **391**, 51 (1998).
[2] S. Perlmutter *et al.*, Astrophys. J. **517**, 565 (1999).
[3] A. G. Riess *et al.*, Astron. J. **116**, 1009 (1998).
[4] M. Tegmark, M. Strauss, and M. Blanton *et al.*, Phys. Rev. D **69**, 103501 (2004).
[5] B. P. Schmidt *et al.*, Astrophys. J. **507**, 46 (1998).
[6] S. Weinberg, Rev. Mod. Phys. **61**, 1 (1989).
[7] P. J. E. Peebles and B. Ratra, Rev. Mod. Phys. **75**, 559 (2003).
[8] P. J. Steinhardt, L. Wang, and I. Zlatev, Phys. Rev. D **59**, 123504 (1999).
[9] M. Malquarti, E. J. Copeland, and A. R. Liddle, Phys. Rev. D **68**, 023512 (2003).
[10] L. Amendola, Phys. Rev. D **62**, 043511 (2000).
[11] A. Sandage, Phys. Today **23**, No. 2, 34 (1970).
[12] E. Hubble, Proc. Natl. Acad. Sci. U.S.A. **15**, 168 (1929).
[13] R. P. Kirshner, Proc. Natl. Acad. Sci. U.S.A. **101**, 8 (2004).

[14] A. G. Riess *et al.*, Astrophys. J. **826**, 56 (2016).
[15] G. Hinshaw *et al.*, Astrophys. J. Suppl. Ser. **208**, 19 (2013).
[16] Planck Collaboration, Astron. Astrophys. **594**, A13 (2016).
[17] D. J. Fixsen, Astrophys. J. **707**, 916 (2009).
[18] J. L. Sievers *et al.*, J. Cosmol. Astropart. Phys. 10 (2013) 060.
[19] J. R. Gott, M. S. Vogeley, S. Podariu, and B. Ratra, Astrophys. J. **549**, 1 (2001).
[20] S. Podariu, T. Souradeep, J. R. Gott III, B. Ratra, and M. S. Vogeley, Astrophys. J. **559**, 9 (2001).
[21] G. Chen and B. Ratra, Publ. Astron. Soc. Pac. **115**, 1143 (2003).
[22] S. Crandall and B. Ratra, Astrophys. J. **815**, 87 (2015).
[23] S. Crandall and B. Ratra, Phys. Lett. B **732**, 330 (2014).
[24] X. Ding, M. Biesiada, S. Cao, Z. Li, and Z.-H. Zhu, Astrophys. J. **803**, L22 (2015).
[25] O. Farooq and B. Ratra, Astrophys. J. **766**, L7 (2013).
[26] G. Chen and B. Ratra, Publ. Astron. Soc. Pac. **123**, 1127 (2011).
[27] Y. Chen and B. Ratra, Phys. Lett. B **703**, 406 (2011).
[28] R. Jimenez and A. Loeb, Astrophys. J. **573**, 37 (2002).
[29] Z.-E. Liu, H.-R. Yu, T.-J. Zhang, and Y.-K. Tang, Phys. Dark Universe **14**, 21 (2016).
[30] V. V. Lukovic, R. D'Agostino, and N. Vittorio, Astron. Astrophys. **595**, A109 (2016).
[31] J. P. Zibin, Phys. Rev. D **78**, 043504 (2008).
[32] J. P. Zibin, Phys. Rev. D **84**, 123508 (2011).
[33] W. Valkenburg, V. Marra, and C. Clarkson, Mon. Not. R. Astron. Soc. **438**, L6 (2014).
[34] M. Zumalacarregui, J. Garcia-Bellido, and P. Ruiz-Lapuente, J. Cosmol. Astropart. Phys. 10 (2012) 009.
[35] M. Tokutake, K. Ichiki, and C.-M. Yoo, arXiv:1712.04229.
[36] O. Farooq, F. R. Madiyar, S. Crandall, and B. Ratra, Astrophys. J. **835**, 26 (2017).
[37] M. Goliath and G. F. R. Ellis, Phys. Rev. D **60**, 023502 (1999).
[38] B. Saha, Mod. Phys. Lett. A **20**, 2127 (2005).
[39] H. Amirhashchi, Astrophys. Space Sci. **351**, 641 (2014).
[40] M. Betoule *et al.*, Astron. Astrophys. **568**, A22 (2014).
[41] J. T. Nielsen, A. Guffanti, and S. Sarkar, Sci. Rep. **6**, 35596 (2016).
[42] D. Blas, J. Lesgourgues, and T. Tram, J. Cosmol. Astropart. Phys. 07 (2011) 034.
[43] B. Audren, J. Lesgourgues, K. Benabed, and S. Prunet, J. Cosmol. Astropart. Phys. 02 (2013) 001.
[44] https://github.com/cmbant/getdist.
[45] P. A. R. Adel *et al.*, Astron. Astrophys. **594**, A13 (2016).
[46] E. Aubourg *et al.*, Phys. Rev. D **92**, 123516 (2015).
[47] G. Efstathiou, Mon. Not. R. Astron. Soc. **440**, 1138 (2014).
[48] H. Akaike, IEEE Trans. Autom. Control **19**, 716 (1974).
[49] H. S. Jeffreys, *Theory of Probability*, The International Series of Monographs on Physics (Clarendon Press, New York, 1983).
[50] H. Wang and T.-J. Zhang, Astrophys. J. **748**, 111 (2012).
[51] D. Spergel *et al.*, Astrophys. J. Suppl. Ser. **148**, 175 (2003).